Korean J. Chem. Eng., 32(12), 2473-2483 (2015)
DOI: 10.1007/s11814-015-0114-y

pISSN: 0256-1115
eISSN: 1975-7220

A new efficient empirical correlation for filtrate flux in slurry bubble column reactor of a gas-to-liquid process

Mohammad Reza Hemmati*,† and Mohammad Ali Khodagholi**

*Entekhab Petrochemical Co. No. 8, Alley 6, Khaled Eslamboli (Vozara) Street, Tehran, Iran
**Gas Conversion Technologies Group, Gas Processing and Transmission Technologies Research Division, Research Institute of Petroleum Industry (RIPI), West Blvd. Azadi Sport Complex, P. O. Box 14665-137, Tehran 1485733111, Iran
(*Received 9 June 2014 • accepted 30 May 2015*)

Abstract−Gas to Liquid has recently become of great interest. In this technology slurry bubble column reactors are favored for many reasons. Separation of liquid wax from the slurry is still a major problem that may be done by internal or external filtration. A system of sintered metal candle filters are designed and operated to collect experimental data of internal filtration. Data for 4 and 8 micron filter elements with different pressure differences and kinematic viscosity were collected. Data analysis revealed that these data could be correlated as a simple function of time, pressure drop and kinematic viscosity. This new and efficient correlation shows excellent ability to reproduce original data at moderate filtration conditions, but it is less precious in severe conditions. It was understood that main reason for this behavior is different filtrate flux regimes through filter media pores, led to inability of a single correlation to fit both regimes properly.

Keywords: Gas to Liquid (GTL), Internal Filtration, Sintered Metal Filter Elements, Empirical Correlation

INTRODUCTION

XTL (Anything to Liquid) is a phrase that represents all technologies intended to convert any source of carbon to liquid hydrocarbons. These processes have at least three main steps: syngas production, Fischer Tropsch Synthesis (FTS) and product finalizing. The syngas production step converts source of carbon to mixture of hydrogen and carbon monoxide [1-5]. In FTS unit syngas is converted to different hydrocarbons such as paraffin, olefin, oxygenated, etc., by use of suitable iron or cobalt based catalysts which is the most important part of any XTL factory. Finally, the hydrocarbon products might undergo some finalizing steps to reach the required specifications of the market that is the last step of any XTL process and may be done via different technologies such as hydrocracking and thermal cracking [6,7].

Among all of the XTL routes coal to liquid (CTL) and gas to liquid (GTL) are industrially and commercially well-known and more utilized, and hence more important. CTL has an old historical background that goes back to 1932 in Germany and today it is still in operation in China and South Africa. GTL is more well-known because of its industrial application in huge production rates in Pearl [8] and Oryx (both in Qatar), Mossel bay (South Africa) and Bintulu (Malaysia) and some planned units in Iran, Algeria and … [8,9]. In other words, although a pipeline is a routine method for natural gas transmission in countries with huge amounts of this asset [10], GTL also has its own value in monetizing natural gas source to easily vendible liquid hydrocarbons and many studies are devoted to different fields of GTL process such as process simulation and modeling [11], proper process selection [12], effect of product distribution on the economy of production process, and catalysts. Amongst these fields the catalyst is more attractive from different points of view such as promoters and formulation, support, and preparation [13]. Also GTL can serve as a suitable route to utilize CO_2, the world most produced greenhouse gas, to reduce negative environmental effects and help achieve sustainable development [14].

Reactor design is of high importance too. There are different types of reactors to perform FTS such as multi-tubular fixed bed reactors, slurry bubble column reactors (SBCR), fluidized bed and circulating fluidized bed reactors [9,15]. Although each reactor has its own advantages, the ease of performance and manufacture, high production rates and other technical and economic issues make the SBCR a suitable choice for the FTS [9].

Beside many features of SBCRs, wax/catalyst separation in these reactors is still troublesome and no useful documents or design procedures are available in the public domain to design a proper separation system. For example there are many documents relevant to new support materials such as carbon nano tubes (CNT) which make it possible to efficiently control cobalt particle size [16]. Intrinsic kinetics and finding kinetic parameters of FTS reaction are other attractive issues which are very important for reactor design [17, 18]. But it is almost impossible to find a proper, efficient and suitable correlation for correct estimation of filtrate flux during separation of the liquid wax product from the slurry inside the reactor.

†To whom correspondence should be addressed.
E-mail: mrz_hemmati@yahoo.com, m.hemmati@enpetro.com
‡This research was done in RIPI (Research Institute of Petroleum Industry) and by their financial supports.

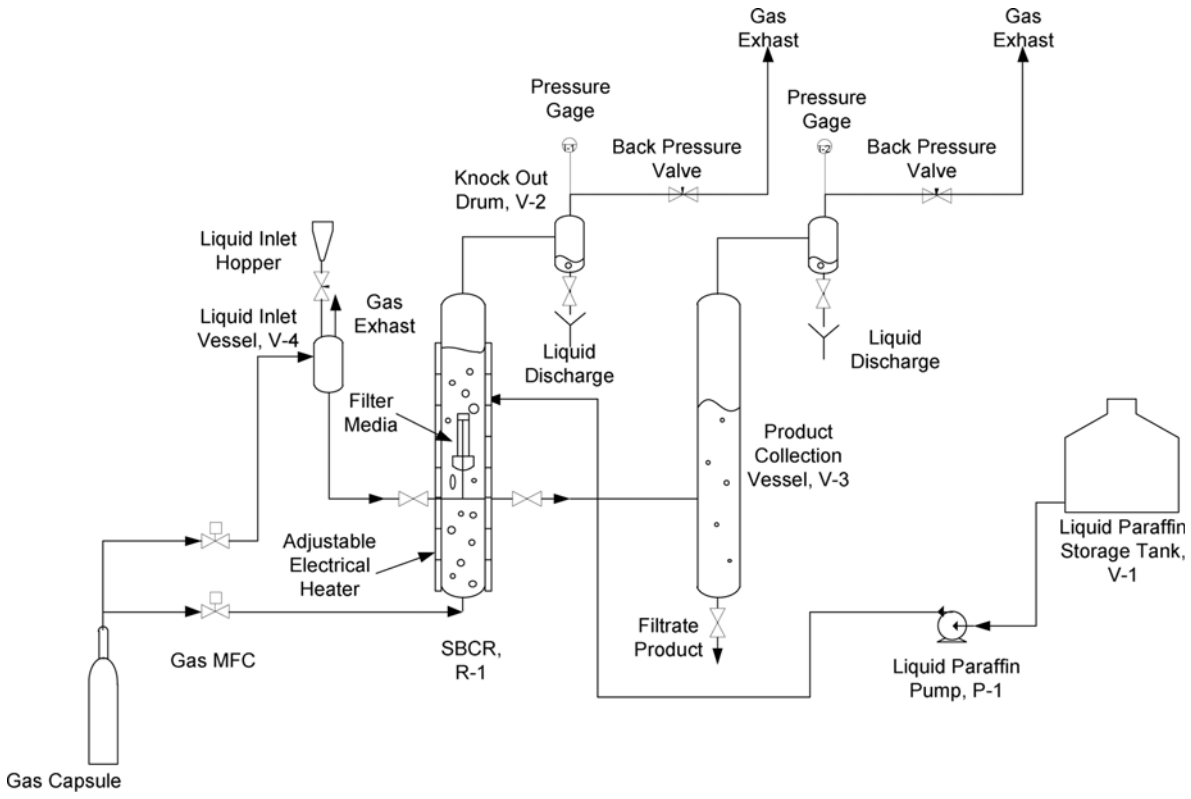

Fig. 1. Schematic flow diagram of the bench scale internal filtration setup.

Wax/catalyst separation could be done by different routes such as internal and external filtration, vacuum distillation, thermal cracking of wax, sedimentation, centrifugal equipment (hydroclone and centrifuge), solvent assisted techniques, magnetic separation and chemical methods [19]. Amongst these routes internal filtration is more suitable for SBCRs since it is easily implemented and requires less process equipment. As it was stated before, there are apparently few documents in the field of wax-slurry separation using internal filters. This may be a result of high-tech essence of this filtration and a need for a multidisciplinary design that is exclusively done by some professional companies, with their in-house documents.

The present work investigates the effect of kinematic viscosity (ν), pressure difference (ΔP) and time (t) on the rate of internal filtration. An experimental setup was designed and operated to collect empirical data in different operating conditions and time. There is not any evidence of design or operation of such an apparatus up to this date. The most interesting part of the present investigation is fitting of the data with 16 different models. This part is new again since no correlations for estimation of filtrate flux have been introduced. All models are simple linear correlations of filtrate flux (Q) versus natural logarithm of time, but the coefficients of these models are simple or complex correlations of pressure difference (ΔP) and kinematic viscosity or ΔP and temperature (T). The results reveal that a set of ΔP and ν are favored over ΔP and T. Also, all models fail to reproduce original data at severe filtration conditions of high viscosity and low ΔP. The reason is the change of the flow regime through filter media.

EXPERIMENTAL

Experiments were performed in a bench scale setup, illustrated schematically in Fig. 1. Pure and clear liquid paraffin is supplied from vessel V-1 to the reciprocating pump P-1. The pump is acted by an electronic command of a level controller to certify constant level of slurry inside the SBCR (R-1). Liquid paraffin is routed to SBCR (R-1) via 3/8 inch tube and enters the reactor in the middle part. The R-1 is a 4 inch diameter vessel of 3 meters length divided into two sections by middle flanges. A gas flow (normally air or nitrogen) is supplied from capsules with pressure control through a regulating valve. The flow of this gas stream is controlled via mass flow controller (MFC, Model: 5850, by Brooks Instruments) and then enters into the reactor in the lowest part through a perforated distributer, namely sparger. This stream is used to prepare a three phase mixture that is similar to the actual SBCR conditions. The flow regime inside the SBCR is directly affected by this stream. In low flow rates the prevailing regime is homogeneous bubble flow. In higher flow rates and, especially, diameters higher than 15-30 cm, the flow regime shifts to churn turbulent. In moderate flow rates another flow regime may prevail, namely slug, with large bubbles that occupy all the cross section of the column. Transition between these regimes is not abrupt, and a transition regime with properties of both regimes exists in between [20].

The gas stream is distributed inside the reactor and commingled with the existing slurry of paraffin and solid particles. Solid particles are selected as a particular type of aluminum oxide with apparent density and shape similar to the real cobalt catalyst. The

filter element is placed in the 1/3 middle length from the lower part of the R-1. Gas bubbles after traveling the length of the slurry level in the R-1 are separated from the top of the slurry and rise through the remaining length to reach the exit point at the top of the vessel. This gas flow stream, before being exhausted to the atmosphere, is routed to a knock out drum (V-2) which separates fine droplets of entrained liquid and collects them for intermittent manual discharge. This setup is equipped with a back-pressure controlling valve that controls the pressure of the R-1. Temperature of the slurry inside the SBCR was controlled by an adjustable electrical heater worn around the external surface of the reactor.

Filtrate product that is extracted from the slurry via filter media is routed to another vessel, V-3. This vessel is also pressurized with a pressure controlled gas stream. V-3 pressure control is important because the pressure difference along the filter media was maintained via pressure of this vessel. This pressure control is also done by using a back-pressure controlling valve and reading the installed pressure gage. V-3 has enough volume to collect all of the filtrate produced during a test period.

It is a common practice to backwash the filter media in the cake filtration to restore the initial capabilities of the filter media. A liquid paraffin stream is responsible for this task. Liquid paraffin was poured into the V-4 vessel. Then this vessel was pressurized by a stream of gas to reach the adequate pressure; the pressure of V-4 is monitored via a pressure gage and manually controlled on 1-1.2 bars more than R-1 pressure by a back-pressure valve. This limited pressure drop is to ensure safe distance from dangerous range of pressure difference (about 2 bars), which led to collapse of sintered metal filter media. Then, while the gas entering stream exists, a ball valve between V-4 and R-1 quickly opens. So a sudden stream of paraffin enters the filter media and causes the filter cake on its external surface to be removed.

Filter elements are candle type sintered metal and are cylindrical. The filter elements have different pore size of 4 and 8 microns. To perform the experiments, first a perforated support is prepared by a piece of stainless steel tube. Then, two heads for front and end sides of the element are prepared by a proper type of stainless still sheet and the perforated support tube is welded to the end head. The front head is perforated and a threaded pipe is welded to the external surface of this head; the perforated support tube is installed in the internal side of this front head by threaded connections to provide a suitable route from this support tube to the discharge connection. By this design it is possible to replace the filter element after opening the threaded connection of the support tube from the front end. For sealing the filter media in its place, suitable Teflon gaskets were prepared and installed between the filter element and both front and end heads. Fig. 2 demonstrates the design of a candle filter element.

We applied this design before for making other experiments and now it is developed in some aspects of the process; also some technical delicacies were solved to reach better operation. For example, it was deduced that utilization of a gas stream for backwashing is not suitable, or filling the V-4 vessel with the pump is not recommended since the exact amount of liquid could not be estimated [21,22].

Viscosity was measured by a Townson+Mercer, Series IV (England) with ASTM D445 method. Viscosity of liquid paraffin was measured at two temperatures, 40 and 100 °C, and extrapolated or interpolated with ASTM D341 method to other temperatures.

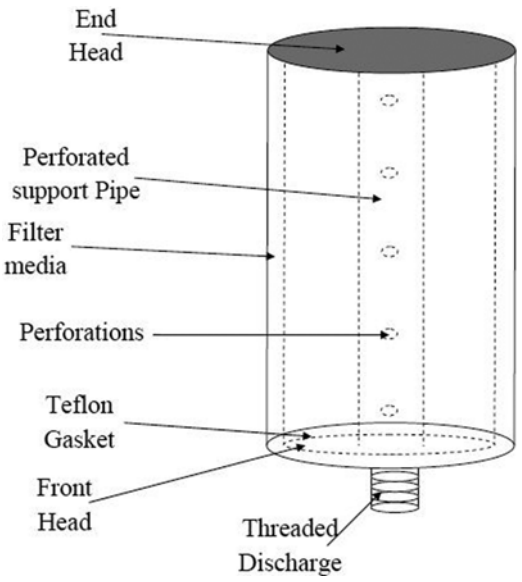

Fig. 2. Scheme of filter element design.

RESULTS

It is common practice to perform cake filtration under constant ΔP or perhaps constant filtrate flux. Constant flux mode is harder to achieve and less attractive in industrial operations [23]. Also, reaching a constant flux requires alternating the ΔP across the filter elements, but the applied sintered metal filter elements are sensitive to high ΔP and hence it is not logical to decrease the downstream pressure of the filter element to reach higher ΔP. Considering all of these items led us to select constant ΔP condition for the experiments.

Flux in a typical cake filtration application is influenced by many parameters. These parameters are classified in three main categories as geometric variables (for filter media such as dimensions, pore size and pore size distribution, for the system such as type of design, diameter of column, piping system, pump for backwashing and …, geometric properties of solid particles such as particles size and particle size distribution, shape, …) operating condition (P, ΔP, T, Level, flow and flow regime, number of interacting phases …) and physicochemical properties (density of liquid, solid and gas, viscosity of liquid, surface tension of liquid …). Some of these factors are fixed and predefined in a particular filtration; for example, in the GTL process, size, shape and properties of solid particles are predefined by the catalyst and reactor conditions. Also, operating pressure, temperature and flow regime are fixed too for the same reason. Constant value of operating conditions led to constant value of physical properties. Variable parameters are those relevant to filter media and also DP which is more important. In the present investigation four levels of ΔP were applied as 0.3, 0.5, 0.75 and 0.9 bar.

Although GTL wax is a complex mixture of different hydrocar-

Table 1. Viscosity of applied paraffin versus temperature

Temperature (k)	Kinematic viscosity of paraffin (cSt or mm^2/s)	Method of data preparation
288	29.01	Extrapolated
295	20.59	Extrapolated
305	14.36	Extrapolated
313	11.13	Exact value
315	10.49	Interpolated
325	7.95	Interpolated
335	6.22	Interpolated
345	5.00	Interpolated
373	3.02	Exact value

bons, physicochemical properties of this material may be estimated closely by assuming this cut as normal C28 paraffin ($C_{28}H_{58}$) [24, 25]. By this assumption kinematic viscosity of GTL wax in temperature ranges between 120 (the lowest possible temperature for filtration operation, which is related to external filtration) to 230 °C (the highest operating temperature of the SBCR, for internal filtration) is about 0.5 to 2.5 cSt. Although the actual kinematic viscosity of the applied paraffin sample (which is not $C_{28}H_{58}$, but instead it is a proper paraffin which is in liquid state at room temperature) was above this range (Table 1), the results are valuable from different points of view. The most important of them is extrapolation possibility. By this method, a few points in a certain viscosity were analyzed experimentally and results were compared with the model. If the error is in the acceptable range, it is recommended to use the generalized correlation for all states of that viscosity without performing the whole experiments. Other benefit of this study is to assure the possibility of applying such apparatus for making wax/catalyst separation. In other words, when this filtration system composed of sintered metal filter elements and the prevailing concepts of operation are capable of making the anticipated separation, it is definitely possible to apply it in easier separations such as less viscous liquids. So it is possible to use this apparatus in the present or other sizes to appraise filtration capability of other paraffin resembling liquids with more similar viscosity. Also, the experimental results of the present investigation led to correlations that are useful for future studies by providing ideas for the form of generalized correlation, range of coefficients, acceptable error ranges, etc. Note that viscosity data in Table 1 are categorized as exact value, interpolated and extrapolated. Exact values are extracted directly from laboratory but extrapolated and interpolated data are calculated based upon ASTM D341 method by use of exact values at 313 and 373 k.

Also note that there is an initial clogging of ultra-fine pores in first application of the filter elements [21,22]. This phenomenon is attributed to the existence of very fine particles that are a product of catalyst attrition. These fine particles diffuse through fine pores and cause permanent blockage of them. This phenomenon is more meaningful in the first filtration cycle, causing the initial filtrate flux to fall rapidly from a high initial amount to an equilibrium value. After development of the cake on the external surface of the filter media (and first backwashing), it is not possible to reach the

Table 2. Filtrate flux versus time (min), kinematic viscosity (mm^2/sec) and ΔP (bar) for 4 micron filter element

ΔP →		0.3 bar	0.5 bar	0.75 bar	0.9 bar
Kinematic viscosity (ν)	Time	Flux	Flux	Flux	Flux
29.01	15	0.511	1.075	1.586	2.188
29.01	30	0.420	0.869	1.424	1.543
29.01	45	0.355	0.822	1.309	1.376
29.01	60	0.311	0.774	1.232	1.271
29.01	75	0.263	0.740	1.156	1.199
29.01	90	0.215	0.702	1.113	1.132
29.01	120	-	0.664	1.075	1.089
29.01	150	-	-	-	1.041
20.59	15	1.338	2.742	3.201	4.562
20.59	30	1.070	2.446	2.580	3.879
20.59	45	1.018	2.322	2.288	3.654
20.59	60	0.951	2.202	2.092	3.497
20.59	75	0.898	2.140	1.868	3.454
20.59	90	0.855	2.092	1.696	3.396
20.59	120	0.836	2.059	1.505	3.306
14.36	15	2.111	2.990	3.268	5.111
14.36	30	1.873	2.785	2.627	4.505
14.36	45	1.739	2.680	2.331	3.874
14.36	60	1.553	2.618	1.968	3.764
14.36	75	1.505	2.527	1.796	3.602
14.36	90	1.438	2.465	1.610	3.511
14.36	120	-	2.398	1.443	3.416
10.49	15	2.604	3.172	3.664	5.298
10.49	30	2.006	2.971	3.177	5.035
10.49	45	1.849	2.818	2.924	4.720
10.49	60	1.753	2.780	2.651	4.624
10.49	75	1.658	2.752	2.489	4.529
10.49	90	1.624	2.728	2.326	4.443
10.49	120	1.596	2.685	2.116	4.371
10.49	150	1.490	-	-	-
7.95	15	2.604	3.831	4.658	6.769
7.95	30	2.121	3.511	4.185	6.473
7.95	45	2.078	3.287	3.879	6.220
7.95	60	1.963	3.186	3.664	6.153
7.95	75	1.873	3.100	3.497	6.048
7.95	90	1.791	3.048	3.396	5.967
7.95	120	1.744	-	3.287	5.881
7.95	150	1.710	-	-	-
6.22	15	2.847	4.682	6.545	9.516
6.22	30	2.651	4.237	5.790	9.134
6.22	45	2.604	4.084	5.513	8.861
6.22	60	2.565	3.941	5.312	8.656
6.22	75	2.522	3.879	5.169	8.541
6.22	90	2.446	3.783	5.035	8.484
6.22	120	2.412	3.740	4.834	8.403
6.22	150	-	3.707	4.720	8.322

initial value of a fresh filter element; instead, an equilibrium value is attained. In the next backwashings, this equilibrium value is almost attainable. Although this physical blockage is more exaggerated for a fresh filter element in the first filtration cycle, it is probable in all filtration cycles. In fact, it is a permanent phenomenon that leads to a gradual decrease of initial flux during each cycle. This is the reason for acid-washing of the filter element after some filtration cycles to restore the initial properties of the filter element. In all of the experiments in the present study, filter elements passed the above-mentioned initial filtrate flux depression.

For each filter media in different ΔP, test runs were performed in specific temperatures, and the results of filtrate flux versus time and ΔP in particular dynamic viscosities are reported in Tables 2 and 3 for four and eight micron filter elements, respectively. It is also possible to illustrate all of these data on graphs representing Q versus time in constant ΔP and kinematic viscosities. Trend of filtrate decrease with time is similar with that presented in Table 2 for other data, but obviously the slope and intercept of the curves are unique for each condition.

Table 3. Filtrate flux versus time (min), kinematic viscosity (mm^2/sec) and ΔP (bar) for 8 micron filter element

ΔP →		0.3 bar	0.5 bar	0.75 bar	0.9 bar
Kinematic viscosity (ν)	Time	Flux	Flux	Flux	Flux
20.59	15	1.338	2.742	3.201	4.562
20.59	30	1.070	2.446	2.580	3.879
20.59	45	1.018	2.322	2.288	3.654
20.59	60	0.951	2.202	2.092	3.497
20.59	75	0.898	2.140	1.868	3.454
20.59	90	0.855	2.092	1.696	3.396
20.59	120	0.836	2.059	1.505	3.306
14.36	15	2.111	2.990	3.268	5.111
14.36	30	1.873	2.785	2.627	4.505
14.36	45	1.739	2.680	2.331	3.874
14.36	60	1.553	2.618	1.968	3.764
14.36	75	1.505	2.527	1.796	3.602
14.36	90	1.438	2.465	1.610	3.511
14.36	120	-	2.398	1.443	3.416
10.49	15	2.604	3.172	3.664	5.298
10.49	30	2.006	2.971	3.177	5.035
10.49	45	1.849	2.818	2.924	4.720
10.49	60	1.753	2.780	2.651	4.624
10.49	75	1.658	2.752	2.489	4.529
10.49	90	1.624	2.728	2.326	4.443
10.49	120	1.596	2.685	2.116	4.371
7.95	15	2.604	3.831	4.658	6.769
7.95	30	2.121	3.511	4.185	6.473
7.95	45	2.078	3.287	3.879	6.220
7.95	60	1.963	3.186	3.664	6.153
7.95	75	1.873	3.100	3.497	6.048
7.95	90	1.791	3.048	3.396	5.967
7.95	120	1.744	-	3.287	5.881
6.22	15	2.847	4.682	6.545	9.516
6.22	30	2.651	4.237	5.790	9.134
6.22	45	2.604	4.084	5.513	8.861
6.22	60	2.565	3.941	5.312	8.656
6.22	75	2.522	3.879	5.169	8.541
6.22	90	2.446	3.783	5.035	8.484
6.22	120	2.412	3.740	4.834	8.403

DISCUSSION

The main and novel target of this study was to find an empirical correlation that represents all experimental data of a filter media in the whole range of viscosity, ΔP and time. Although filtration rate is generally a function of other parameters (such as solid properties, particles size and size distribution, filter media material and porosity, liquid density, surface tension, and geometry of the apparatus), in a specific operation like this, those are almost or quite constant. Hence, the most important independent variables that affect filtration rate are ΔP, time and kinematic viscosity. On the other hand, viscosity is temperature-dependent, so the functionality of filtrate flux to kinematic viscosity may also be replaced by temperature. This correlation is used for interpolation between data points or even extrapolation beyond experimental range of independent variables. The benefit of such arithmetic correlation is more sensible in modeling of an SBCR, when it is not possible to deal with a huge amount of experimental data. So the simulator or model developer can use simple or complex correlations that represent all points to reproduce them.

It is obvious that changing the filter media leads to a completely different situation because of different porosity and its effects on filtrate flow through the pores of media and also blockage behavior of pores. So for each filter media an individual correlation should be developed.

As stated above, filtrate flux is a function of kinematic viscosity, time and ΔP. This is simply shown as:

$$Q=Q(t, \nu, \Delta P) \quad (1)$$

Also, kinematic viscosity is a strong function of temperature. Hence, this equation can be rewritten as:

$$Q=Q(t, T, \Delta P) \quad (2)$$

Although there are many possibilities for the shape of these correlations, a simple and useful format is utilized here. Eq. (3) shows the proposed correlation format of the present study.

$$Q=m\times\ln(t)+h \qquad m \text{ and } h=f(\nu, \Delta P) \text{ or } f(T, \Delta P) \quad (3)$$

This format is proposed for several reasons. First, the time dependency of filtrate flux in all experiments was the same, and in all occasions it was best fitted by a natural logarithm function. It is possible to correlate slope and intercept of Eq. (3) with ΔP and ν or T, as independent variables and testing the capability of such model for reproducing all data points. So there are two occasions for independent variable sets of m (slope) and h (intercept): ΔP and ν; and ΔP and T. Also, investigations revealed that although complex correlations show superior behavior in modeling of experimental results, sometimes less complicated correlations might lead

Table 4. Slope and intercept of different models

	m=m (ΔP, ν) SC	m=m (ΔP, ν) CC	m=m (ΔP, T) SC	m=m (ΔP, T) CC	h=h (ΔP, ν) SC	h=h (ΔP, ν) CC	h=h (ΔP, T) SC	h=h (ΔP, T) CC
Model 1	√				√			
Model 2	√					√		
Model 3	√						√	
Model 4	√							√
Model 5		√			√			
Model 6		√				√		
Model 7		√					√	
Model 8		√						√
Model 9			√		√			
Model 10			√			√		
Model 11			√				√	
Model 12			√					√
Model 13				√	√			
Model 14				√		√		
Model 15				√			√	
Model 16				√				√

CC: complex correlation
SC: simple correlation

to similar or even more precise results. These simpler models, decrease calculation efforts considerably and give the possibility of making prompt approximations with a simple calculator instead of a computerized programs, especially in emergency occasions.

Therefore, there are 16 occasions for developing models with different independent variable sets and complexity of the m and h correlations (see Table 4).

The most important part in developing the anticipated model of the present investigation is correlating m and h to the independent variable sets. An important factor is the arithmetic function used for such correlation. Although one can find a correlation that passes exactly through all points, this is not suitable or recommended. The reason is that such model exhibits very unreal and unstable behavior in other points. Figs. 3 and 4 show this issue. Although there is an inherent error in prediction of the available data points in Fig. 4, the shape of the surface ensures that this model is reliable in prediction of other points. On the other hand, the surface of Fig. 3 passes exactly through all data points and there is a little error in their prediction by this model. But the model is inefficient in other points because of the present oscillating behavior. All models of the present study were chosen from a smooth surface similar to Fig. 4.

After evaluation of m and h by the developed models, their capability in reproduction of the experimental data should be appraised.

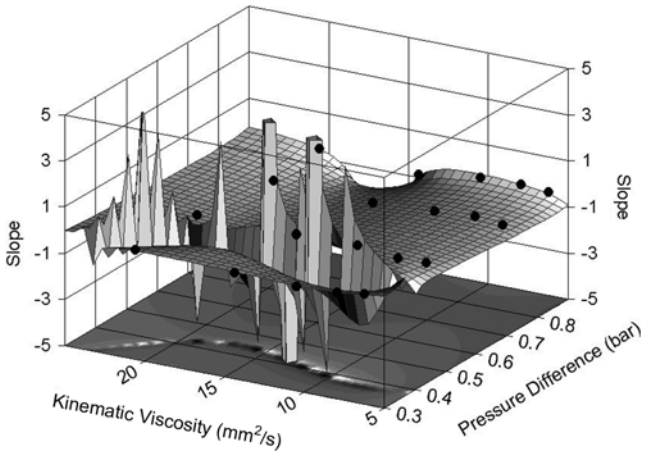

Fig. 3. Arithmetic models that pass exactly through all data points. It leads to a wild and versatile behavior of the model in other points. Shape of the surface shows that this model predicts the value of model slope in other points with high error.

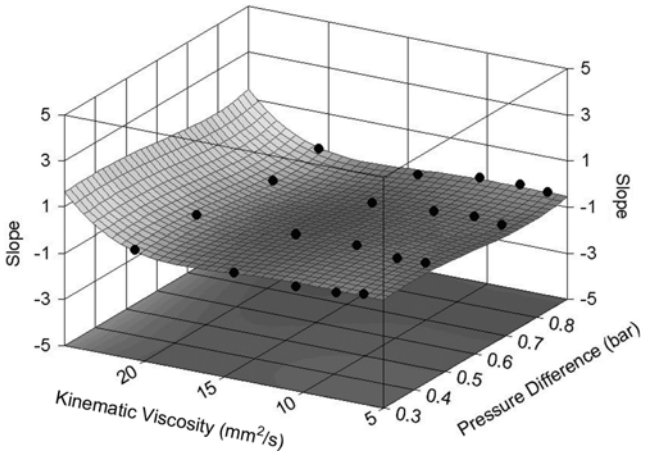

Fig. 4. Although this smooth sample of arithmetic correlations does not pass exactly through all data points, instead it has a fluid and smooth behavior which leads to more reliable data evaluation in points which are not used in model development.

It is obvious that there were errors for each of these 16 models in evaluation of m and h (compared to their exact value). Also, other important error appeared in filtrate flux approximation by Eq. (3). Therefore, it is necessary to compare these models in different fields to find the most appropriate one. For this reason, some important factors were selected among all of the prevailing items:

Absolute value of average error in m, h and Q
Average error in |m|, |h|, and |Q|
Maximum error in |m|, |h|, and |Q|
Minimum error in |m|, |h|, and |Q|

For correct comparison between models, a scoring policy is required. This scoring model is developed by assuming an average acceptable error of 25%, maximum acceptable error of 40% and minimum probable error of 10%. If any model shows an error value less than these amounts, positive points are considered for it based upon the existing difference with the above-mentioned values. On the other hand, if the model leads to more errors, a negative point will be added to the total points of that model. This negative point never exceeds half of the total possible scores (in absolute value) in that item.

This scoring procedure should take into account the relative importance of different errors. It is obvious that the most important item in each model is its capability in correct evaluation of the Q instead of m and h. In another words, it is accepted if some percents of error are included in m and h, but the model has the power to damp these errors in different directions (hence, the flow rate value will be evaluated with moderate error). But this phenomenon is limited and if m and h are evaluated with high errors; in some regions of independent variables there were certainly implemented considerable errors in flow rate prediction. So although it is important to evaluate m and h with a high precision, this is not as important as the capability of the model to give true values of the flow rate. This issue is considered by proper coefficients in Eqs. (4) to (6) for scoring models. In these equations, a coefficient between 0.2 and 0.7 was incorporated to reduce the relative importance of coefficient models score versus score of flow rate evaluation.

$$\text{Model Score}=\text{Coefficient Score}+\text{Approximation Score} \tag{4}$$

$$\begin{aligned}\text{Coefficient Score}=0.7\times\{&(25-[|\text{average (m or h error)}|\\&+\text{average }(|\text{m or h error}|)]/2\}+0.2\\&\times\{40-\text{maximum }(|\text{m or h error}|)\}+0.7\\&\times\{[10-\text{minimum }(|\text{m or h error}|)]\}\end{aligned} \tag{5}$$

$$\begin{aligned}\text{Approximation Score}=3\times(&25-(\text{Average error in }\Sigma|Q|\\&+|\text{Average error in }\Sigma Q|)/2)\\&+(40-\text{Maximum error in }\Sigma|Q|)+2\\&\times(10-\text{Minimum error in }\Sigma|Q|)\end{aligned} \tag{6}$$

By these equations, a model can gather a maximum of 200 scores (two individual 32.5 scores for m and h and a 135 score for Q) and minimum of −100 (half of maximum possible scores).

Results for this comparison are reported in Tables 5 and 6 for four and eight micron filter elements.

Evaluation of m and h for 4 micron filter media reported here.

m as a complex correlation of ΔP and ν:

$$m=a+b\times\Delta P+c\times\Delta P^2+d\times\Delta P^3+e\times\Delta P^4+f\times\Delta P^5+g\times\nu+h\times\nu^2+i\times\nu^3+j\times\nu^4$$

a=−0.27, b=3.302, c=1.66, d=−14.17, e=5.46, f=5.07,
g=−0.38, h=0.061, i=−0.0041, j=9.14e-05

m as a simple correlation of DP and noo.

$$m=a+b\times\ln\Delta P+c/\nu$$

a=−0.755, b=−0.341, c=0.54

m as a complex correlation of ΔP and T:

$$m=a+b\times\Delta P+c\times\Delta P^2+d\times\Delta P^3+e\times\Delta P^4+f/T+g/T^2+h/T^3$$

Table 5. Comparison between models for 4 micron filter

	Coefficient score (m)	Coefficient score (h)	Total coefficient score	Interpolation score	Final score
Model 1	4.14	16.68	20.82	35.80	56.62
Model 2	4.14	15.58	19.72	30.50	50.22
Model 3	4.14	16.03	20.17	30.75	50.92
Model 4	4.14	7.64	11.78	−17.7	−5.92
Model 5 (*)	12.51	16.68	29.19	46.75	75.94
Model 6	12.51	15.58	28.09	46.65	74.74
Model 7	12.51	16.03	28.54	43.3	71.84
Model 8	12.51	7.64	20.15	−13.2	6.95
Model 9	4.17	16.68	20.85	35.1	55.95
Model 10	4.17	15.58	19.75	30.3	50.05
Model 11	4.17	16.03	20.2	30.25	50.45
Model 12	4.17	7.64	11.81	−18.05	−6.24
Model 13	13.27	16.68	29.95	31.5	61.45
Model 14	13.27	15.58	28.85	28.4	57.25
Model 15	13.27	16.03	29.3	26.9	56.2
Model 16	13.27	7.64	20.91	−37.7	−16.79
Average	8.52	13.98	22.51	20.60	43.10
Minimum	4.14	7.64	11.78	−37.7	−16.79
Maximum	13.27	16.68	29.95	46.75	75.94

Table 6. Comparison between models for 8 micron filter

	Coefficient score (m)	Coefficient score (h)	Total coefficient score	Interpolation score	Final score
Model 1	−0.49	16.47	15.98	37.93	53.91
Model 2	−0.49	16.90	16.41	31.38	47.79
Model 3	−0.49	17.03	16.54	38.89	55.43
Model 4	−0.49	14.37	13.88	22.63	36.51
Model 5 (*)	14.67	16.47	31.14	50.08	81.22
Model 6	14.67	16.90	31.57	49.55	81.12
Model 7 (**)	14.67	17.03	31.7	49.53	81.23
Model 8	14.67	14.37	29.04	33.56	62.6
Model 9	−0.68	16.47	15.79	38.03	53.82
Model 10	−0.68	16.90	16.22	30.99	47.21
Model 11	−0.68	17.03	16.35	38.54	54.89
Model 12	−0.68	14.37	13.69	22.35	36.04
Model 13	12.92	16.47	29.39	34.89	64.28
Model 14	12.92	16.90	29.82	33.67	63.49
Model 15	12.92	17.03	29.95	35.90	65.85
Model 16	12.92	14.37	27.29	10.60	37.89
Average	−6.61	16.19	22.80	34.91	57.71
Minimum	−0.68	14.37	13.69	10.6	36.04
Maximum	14.67	17.03	31.7	50.08	81.23

**The best model with the highest score
*This model seems as perfect as model 7 since its cores is just 0.01% less that that model

a=−671.69, b=−37.23, c=114.67, d=−149.57, e=68.71, f=640170, g=−2.02e+08, h=2.12e+10

m as a simple correlation of ΔP and T:

$m=a+b\times\ln\Delta P+c/T$
a=−0.755, b=−0.34, c=0.54

h as a complex correlation of ΔP and ν:

$h^{-1}=a+b\times\ln\Delta P+c/\nu^{0.5}+d/\nu+e\times\ln\nu/\nu^2$
a=3.25, b=−0.15, c=−35.07, d=123, e=−188.

h as a simple correlation of ΔP and ν:

$h^{-1}=a+b/\Delta P^{0.5}+c/\nu^2$
a=−0.08, b=0.24, c=−2.91

h as a complex correlation of ΔP and T:

$h^{-1}=a+b\times\Delta P+c\times\Delta P^{0.5}+d\times T^2+e\times T^2\times\ln T+f\times T^3+g\times\exp(T)$
a=976.07, b=0.28, c=−0.84, d=−0.412, 27, e=0.08, 4295, f=−0.00021, g=2.31

h as a simple correlation of ΔP and T:

$h^{-1}=a+b\times\ln\Delta P+cT^2$
a=0.42, 44, b=−0.16, c=−3.02e-06,

Equations for 8 micron filter element:

m: Complex Correlation of ΔP and ν

$m=a+b\times\Delta P+c\times\Delta P^{1.5}+d\times\Delta P^{0.5}+e\times e^{-\Delta P}+f\times\nu+g\times\nu\times\ln\nu+h\times\nu^{0.5}\times\ln\nu+i\times(\ln\nu)^2$
a=1305, b=−680, c=315, d=94.9, e=−456.619, f=-929, g=117.30, h=931, i=−200.

m: Simple Correlation of ΔP and ν

$m=a+b\times\Delta P+c/\nu$
a=−0.19, b=−0.63, c=0.70

m: Complex Correlation of ΔP and T

$m=a+b\times\Delta P+c\times\Delta P^2+d\times\Delta P^3+e\times\Delta P^4+f/T+g/T^2+h/T^3$
a=−504, b=−24.14, c=81.84, d=−114.93, e=55.56, f=481384, g=−1.53e+08, h=1.61e+10

m: Simple Correlation of ΔP and T

$m=a+b\times\ln\Delta P+c\times T$
a=−0.70, b=−0.63, c=0.0019

h: Complex Correlation of ΔP and ν

$h^{-1}=a+b\times\Delta P^{1.5}+c\times\Delta P^{0.5}\times\ln\Delta P+d/\nu^{0.5}+e/\nu+f\times\ln\nu/\nu^2$
a=2.32, b=0.82, c=−1.30, d=−33.77, e=118.40, f=−181.07

h: Simple Correlation of ΔP and ν

$h^{-1}=a+b\times\ln(\Delta P)+c/\nu^2$
a=0.15, b=−0.16, c=−2.89

h: Complex Correlation of ΔP and T

$h^{-1}=a+b\times\ln\Delta P+c\times T+d\times T\times\ln T+e\times T/\ln T$
a=1164.07, b=−0.16, c=98.02, d=−6.99, e=−353.68

h: Simple Correlation of ΔP and T

$h^{-1}=a+b\times\ln\Delta P+cT^3$
a=0.31, b=−0.16, c=−6.30e-9,

Tables 5 and 6 reveal that for all circumstances using a complex relation of ΔP and ν for the slope leads to better results. Although in Table 6, Eq. (7) is the best one, Eq. (5) is just a little different from that (about 0.01% difference). In other words, it is possible to expect Eq. (5) as the best model for 8 micron filter element instead of Eq. (7) without meaningful loss of precision. A strong reason for this choice is the occurrence of Eq. (5) as the best equation for 4 micron filter element, so generalization led us to select Eq. (5) for the 8 micron filter too. Also, this model has shown less error in interpolation compared with coefficient evaluation, and as it was stated before, this interpolation is more important than m and h evaluation. Hence, Eq. (5) is the best option for fitting data of both 4 and 8 micron filter element data and reproducing them. This is an important conclusion that temperature is not a proper choice for this data fitting. The reason is a complex nature of temperature dependency of kinematic viscosity. If this is the case, it is really troublesome to include a complex correlation into account.

Other conclusion is that the intercept is almost a simple correlation of ΔP and ν instead of a complex correlation. This might be a result of natural simplicity of this function, or smooth dependency of it in the prevailing range of conditions that is best fitted with a simple correlation.

Another surprising outcome of this data fitting is finding the effect of filtration severity on the model error. Fig. 5, Fig. 6 and Table 7 show the average amount of error for 8 micron filter element. The graphs clearly show that in high viscosity and low ΔP more errors were incorporated into results.

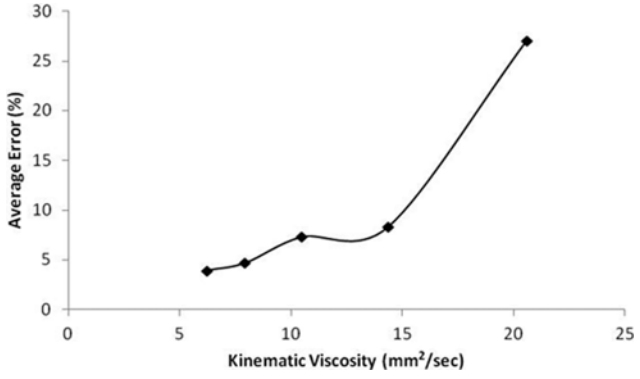

Fig. 5. Dependency of average error to kinematic viscosity.

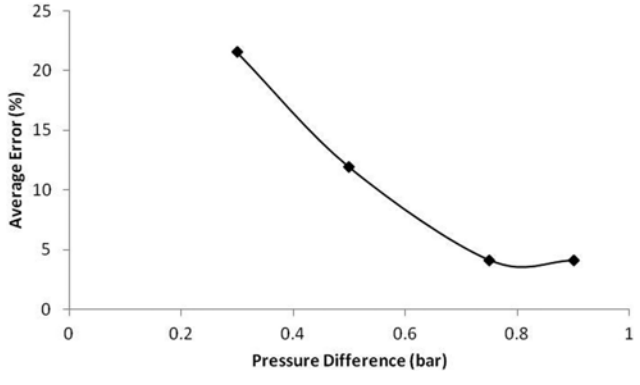

Fig. 6. Dependency of average error to ΔP for 8 micron filter element.

Although these graphs are typical, this behavior is similar for all filter elements. It means that high kinematic viscosity and low pressure drop (which are severe conditions for filtration) are important factors in propagation of error in the model results.

For 8 micron filter, Eq. (5) scores increase from 81.22 to 131.68 by omitting all of data relevant to 20.59 mm^2/sec kinematic viscosity data. In this condition, the average amount of error in the whole range of independent variables was 6.05 with a maximum equal to 23.93. Same trend was repeated for other filter elements (not reported). This issue led to a conclusion about the effect of filtration conditions severity on the efficiency of the models. It is common that high viscosity/low ΔP is a severe condition for filtration that leads to decreasing amount of filtrate flux. All of the present models show inefficiency in these conditions. This inefficiency is so high that none of the presented models succeed to take even half of the total 200 possible score. But by omitting just the highest viscosity data and repeating the calculations, the score of best model increases to about 65% of total possible scores (about 25% improvement). It is common in almost all empirical correlations to introduce a proper range of physical properties for the precise use of that correlation. This range is defined by merely using physical properties or a combination of them as a meaningful dimensionless factor, such as Re, Sc or other well-known parameters. Here the situation is the same and the proposed correlations are suitable for kinematic viscosity less than 14 mm^2/sec.

By these data, it is strongly deduced that in high kinematic viscosities and low pressure differences, when the filtrate flux is low, all models show high errors and inefficiency in reproducing the original data. The reason is changing the prevailing filtration mechanisms consisting of filtrate flow through pores of filter media, compactness of filter cake and its effect on the filtration process and also alteration of flow regime through filter media pores (perhaps). Although it is possible to evaluate macroscopic properties of a filter element in a typical filtration process, that behavior is certainly a result of many interacting differential scale phenomena. It is difficult to take all of them into account, but the visual effect of the resultant vector of all of them was evaluated and fitted by the present models.

CONCLUSION

The most important aim of the present study is to squeeze a huge amount of data in a relatively simple model that is enabled to reproduce the mother data in an acceptable error range, which has not been performed (or reported) before. This was done in a two-step manner, first correlating filtrate flux to time by a linear equation of natural logarithm of time (in constant kinematic viscosity and ΔP) and in the second step correlating the slope and intercept of that model with kinematic viscosity or temperature and ΔP. These correlations could be simple or complex; hence a total of 16 models were introduced for final comparison. A scoring policy also was introduced for comparison between the models. In this scoring model 32.5 scores are considered for true evaluation of m and h, and 135 scores for filtrate flux (totally 200 scores). Also, negative scores are possible up to half of the total scores. Although the cor-

Table 7. Distribution of errors in different conditions for 8 micron filter and Eq. (5)

ΔP →		0.3 bar	0.5 bar	0.75 bar	0.9 bar	
Kinematic viscosity (ν)	Time	Error%	Error%	Error%	Error%	
20.59	15	−58.21	−14.77	−0.44	−3.94	Average (|e%|)=27.07
20.59	30	−76.51	−20.08	−3.73	−12.06	Maximum (|e%|)=78.73
20.59	45	−72.55	−21.22	−3.17	−12.63	Minimum (|e%|)=0.44
20.59	60	−74.76	−23.83	−2.14	−13.02	
20.59	75	−76.84	−24.27	−5.12	−10.75	
20.59	90	−78.73	−24.47	−7.43	−9.56	
20.59	120	−71.53	−22.26	−6.20	−7.61	
14.36	15	10.91	0.94	4.35	7.30	Average (|e%|)=8.32
14.36	30	15.81	3.95	4.49	5.29	Maximum (|e%|)=23.93
14.36	45	19.58	6.45	7.81	−3.00	Minimum (|e%|)=0.21
14.36	60	18.07	8.78	3.80	−0.80	
14.36	75	21.98	9.16	5.63	−1.13	
14.36	90	23.93	9.94	4.78	−0.21	
14.36	120	–	12.39	11.47	2.73	
10.49	15	10.36	−10.66	−5.37	−6.63	Average (|e%|)=7.30
10.49	30	−5.39	−11.33	−4.82	−4.51	Maximum (|e%|)=13.18
10.49	45	−7.43	−13.18	−3.27	−6.70	Minimum (|e%|)=2.58
10.49	60	−8.09	−11.72	−5.56	−5.43	
10.49	75	−10.05	−10.52	−5.58	−4.90	
10.49	90	−8.77	−9.54	−6.95	−4.64	
10.49	120	−5.01	−8.17	−7.16	−2.68	
7.95	15	3.09	−1.30	0.92	−0.27	Average (|e%|)=4.70
7.95	30	−8.34	−4.62	2.55	1.20	Maximum (|e%|)=9.72
7.95	45	−4.25	−8.07	2.96	0.87	Minimum (|e%|)=0.27
7.95	60	−5.57	−8.76	3.35	2.44	
7.95	75	−6.82	−9.62	3.67	2.84	
7.95	90	−8.36	−9.72	4.98	3.25	
7.95	120	−5.96	-	8.58	4.60	
6.22	15	−4.74	−11.08	3.38	−0.06	Average (|e%|)=3.94
6.22	30	−4.82	−10.69	−0.33	−0.19	Maximum (|e%|)=13.01
6.22	45	−2.18	−11.96	0.09	−0.82	Minimum (|e%|)=0.06
6.22	60	−0.41	−11.76	0.34	−1.44	
6.22	75	0.47	−13.01	0.78	−1.41	
6.22	90	−0.46	−13.00	0.83	−0.94	
6.22	120	1.64	−11.94	1.13	−0.09	
Average (|error|)		21.52	11.88	4.09	4.17	
Maximum (|error|)		78.73	24.47	11.47	13.02	
Minimum (|error|)		0.41	0.94	0.09	0.06	

rect evaluation of m and h was important, the most important item is a true evaluation of filtrate flux, so it is possible that a model with low scores for the model coefficients shows acceptable results in evaluation of filtrate flux. This is because sometimes errors propagate in countercurrent direction and lead to a pseudo-correct conclusion. But since this phenomenon is not permanent the individual scores were considered for model coefficients and model exactness.

All of the 16 models were scored. The results revealed that a complex correlation of ΔP and ν is the most appropriate choice for fitting m in all models. The reason is more affinity of the equation to kinematic viscosity instead of temperature. Also, a simple correlation of ΔP and T is more appropriate in correlating h for both 4 and 8 micron filter elements.

It is strongly concluded that in high kinematic viscosities and low pressure differences (when the filtrate flux is low) all models show high errors and inefficiency in reproducing the original data. This is because of changing the prevailing mechanisms of filtration, consisting of filtrate flow through pores of filter media, compact-

ness of filter cake and its effect on the filtration process and perhaps alteration of flow regime through filter media pores.

ACKNOWLEDGEMENTS

The authors would like to express their appreciation for the support rendered by Research and Technology Directorate of National Iranian Oil Company, on the research leading to the present article.

NOMENCLATURE

a to h : correlation coefficients [NA]
m and h : slope and intercept of correlations
t : time [min]
T : temperature [K]
Q : filtrate flux [ml/min/cm^2]
ΔP : pressure difference [bar]
ν : kinematic viscosity [mm^2/sec]

REFERENCES

1. J. J. Marano, *Ene. Proc.*, **1**, 3795 (2009).
2. O. P. R. Van Vliet, A. P. C. Faaij and W. C. Turkenburg, *Energy Convers. Manage.*, **50**, 855 (2009).
3. R. M. Swanson, A. Platon, J. A. Satrio and R. C. Brown, *Fuel*, **89**, S11 (2010).
4. J. L. Casci, C. M. Lok and M. D. Shannon, *Catal. Today*, **145**, 38 (2009).
5. J. R. Rostrup-Nielsen, *Catal. Today*, **71**, 243 (2002).
6. F. A. N. Fernandes and U. M. Teles, *Fuel. Proc. Technol.*, **88**, 207 (2007).
7. A. de Klerk, *Ind. Eng. Chem. Res.*, **46**, 5516 (2007).
8. A. Y. Khodakov, *Catal. Today*, **144**, 251 (2009).
9. A. P. Steynberg and M. E. Dry, Fischer Tropsch Technology, Elsevier (2004).
10. A. Kabirian and M. R. Hemmati, *Ener. Pol.*, **35**, 5656 (2007).
11. X. Hao, M. E. Djatmiko, Y. Xu, Y. Wang, J. Chang and Y. Li, *Chem. Eng. Technol.*, **31**, 188 (2008).
12. C. J. Lee, Y. Lim, H. S. Kim and C. Han, *Ind. Eng. Chem. Res.*, **48**, 794 (2009).
13. M. R. Hemmati, M. Kazemeini, J. Zarkesh and F. Khorasheh, *J. Taiwan Inst. Chem. Eng.*, **43**, 704 (2012).
14. C. Zhang, K. W. Jun, K. S. Ha, Y. J. Lee and S. C. Kang, *Environ. Sci. Technol.*, **14**, 8251 (2014).
15. B. H. *Cat. Today*, **71**, 249 (2002).
16. A. Karimi, B. Nasernejad and A. M. Rashidi, *Korean J. Chem. Eng.*, **29**(11), 1516 (2012).
17. H. Atashi, M. Mansouri, S. H. Hosseini, M. Khorram, A. A. Mirzaei, M. Karimi and G. Mansouri, *Korean J. Chem. Eng.*, **29**(3), 304 (2012).
18. Y. H. Kim, D. Y. Hwang, S. H. Song, S. B. Lee, E. D. Park and M. J. Park, *Korean J. Chem. Eng.*, **26**(6), 1591 (2009).
19. P. Z. Zhou and R. D. Srivastava, Status review of Fischer-Tropsch slurry reactor catalyst/wax separation techniques, Report prepared by Burns and Roe Services Corporation in **1991** for U.S. Department of Energy, Pittsburg Energy Technology Center.
20. A. Behkish, *Hydrodynamic and mass transfer parameters in large-scale slurry bubble column reactors*, Ph. D. Dissertation. University of Pittsburgh (2004).
21. M. A. Khodagholi, M. R. Hemmati and A. Nakhaei-Pour, *Chem. Ind. Chem. Eng. Q.*, **19**(2), 295 (2013).
22. M. A. Khodagholi, A. A. Rohani and M. R. Hemmati, *Internal filter for fischer-tropsch wax/catalyst separation*, Proceeding of FILTECH Conference, 2009, October 13-15, Wiesbaden-Germany.
23. W. L. Mc Cabe, J. Smith and P. Harriot, *Unit operations of chemical engineering*, 7th Ed. McGraw-Hill (2005).
24. K. Pangarkar, T. J. Schildhauer, J. R. van Ommen, J. Nijenhuis, J. A. Moulijn and F. Kapteijn, *Catal. Today*, **147S**, S2 (2009).
25. Y. N. Wang, Y. Y. Xu, H. W. Xiang, Y. W. Li and B. J. Zhang, *Ind. Eng. Chem. Res.*, **40**, 4324 (2001).